

Unexpected periodicity in the quasi-two-dimensional Mott insulator 1T-TaS₂ revealed by angle-resolved photoemission

L. Perfetti,¹ T. A. Gloor,² F. Mila,² H. Berger,³ and M. Grioni¹¹*Institut de Physique des Nanostructures, Ecole Polytechnique Fédérale (EPFL), CH-1015 Lausanne, Switzerland*²*Institut de Théorie des Phénomènes Physiques, EPFL, CH-1015 Lausanne, Switzerland*³*Institut de Physique de la Matière Complexe, EPFL, CH-1015 Lausanne, Switzerland*

(Received 14 January 2005; published 4 April 2005)

High-resolution angle-resolved photoemission data from the insulating phase of the charge-density-wave (CDW) material 1T-TaS₂ reveal the backfolding of the electronic bands associated with the CDW superlattice, but also an additional, unexpected periodicity. This periodicity is consistent with the dispersion predicted at zero temperature if three-sublattice magnetic order is present, suggesting that it is the signature of fluctuations associated with magnetic ordering of a Mott insulator on a triangular lattice.

DOI: 10.1103/PhysRevB.71.153101

PACS number(s): 79.60.Bm, 71.30.+h, 71.10.Fd, 71.45.Lr

Systems of reduced dimensionality—*quasi-one-dimensional* (1D) or *quasi-two-dimensional* (2D)—display a richer variety of electronic instabilities and exotic ground states than their 3D counterparts.¹ In particular, correlation-induced (Mott) metal-insulator (MI) transitions in 1D and 2D are a subject of lingering interest.² Theory has made specific predictions on the properties of the correlated metallic phases,^{3,4} the character of the transition,⁵ and the nature of the magnetic order in the insulating state.⁶ New experiments can now test, in real materials and with increasing accuracy, various aspects of those predictions. Among them, angle-resolved photoemission (ARPES) with high energy and momentum resolution is a direct probe of the electronic bands and of the topology of the Fermi surface. ARPES is sensitive to *k*-dependent changes of the electronic structure across an instability, and to the appearance of new periodicities in the electronic potential in the broken symmetry phases. Moreover, the ARPES line shape carries unique information on the correlations that shape the individual quasiparticles (QPs).⁷

Layered transition metal chalcogenides are valuable 2D model systems where the interplay of electron-phonon interactions and electronic correlations can be investigated. **Electron-phonon coupling, which is often rather strong in these materials, is responsible for charge-density-wave (CDW) instabilities and superconductivity.⁸ In their normal states, the Coulomb interaction energy (*U*) is typically smaller than electronic bandwidths, and chalcogenides should not be considered strongly correlated materials. However, in the CDW phases of 1T-TaS₂ and 1T-TaSe₂, the associated superlattice potential splits the conduction band into narrower subbands, whose widths are comparable with *U*.^{9,10} Electronic correlations then become dominant, and force a MI instability.^{11–15}** In this Brief Report, we present ARPES data on the low-temperature insulating phase of 1T-TaS₂. Thanks to improved experimental conditions, **they reveal the so far elusive effects of the CDW superlattice on the band dispersion, but also a new and unexpected spectral signature which we attribute to fluctuations associated with an underlying magnetically ordered state.**

The 2D electronic character of 1T-TaS₂ is linked to the presence in its structure of infinite Ta planes, where the Ta *d*¹ ions form a triangular lattice. The basic units of the CDW superstructure, which develops below 550 K, are 13-atom “star of David” clusters. In the *commensurate* $\sqrt{13} \times \sqrt{13}$ CDW phase, below *T*_{MI}=180 K, they form a triangular lattice with unit vectors **A**₁=**a**₁+3**a**₂ and **A**₂=4**a**₁−**a**₂, where **a**₁ and **a**₂ are the unit vectors of the original undistorted Ta lattice. The lock-in CDW transition is accompanied by a sudden jump in the electrical resistivity, which is interpreted as a Mott transition within a half-filled CDW subband.⁹ In real space, it corresponds to the localization of one Ta *d* electron at the center of each of the 13-atom stars. Interestingly, and perhaps surprisingly, there is no direct evidence for magnetic order in the insulating phase.

Single crystals of 1T-TaS₂ grown by vapor transport in the form of shiny plaquettes were characterized by x-ray diffraction and transport measurements, which confirmed the crystalline quality and a sharp MI transition, with a characteristic hysteresis. ARPES measurements were performed on specimens freshly cleaved *in situ* at 300 K [room temperature (RT)] and then cooled. We used low-energy electron diffraction to verify the presence of the CDW reconstruction. We utilized 21.2 eV photons from a high-brilliance monochromatized Gammadata He lamp, and a Scienta hemispherical analyzer with energy and momentum resolution Δ*E*=10 meV and Δ*k*=±0.02 Å^{−1}, respectively. The Fermi level position was determined with an accuracy of ±1 meV by measuring the metallic cutoff of a polycrystalline Ag film. The data were reproduced on various surfaces, but we found that the visibility of the weak superlattice bands strongly depends on the perfection of the cleaved surface.

The ARPES intensity map of Fig. 1(a) summarizes RT data along the high-symmetry Γ M direction. A broad (1 eV) Ta *d*_{z²} band disperses upwards from the zone boundary, and crosses the Fermi level at *k*_F~0.25 Γ M, in good agreement with previous ARPES data,^{14–16} and with band-structure calculations.¹⁰ The top of the *S* *sp* band is visible at ~1.2 eV at Γ . Photon-energy-dependent measurements at normal emission (not shown), which probe the Γ A direction perpen-

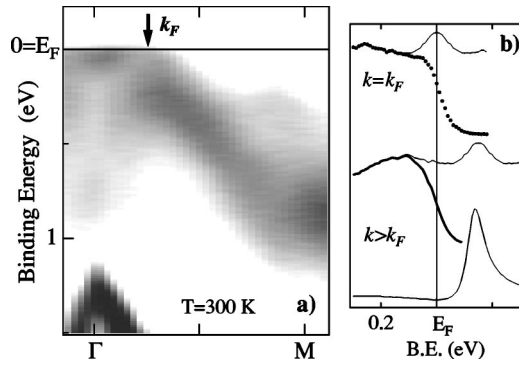


FIG. 1. (a) ARPES intensity map of 1T-TaS₂ measured in the metallic state (300 K) along the Γ M high-symmetry direction ($h\nu=21.2$ eV). The arrow marks the Fermi level crossings by the Ta *d* band. (b) (top) The spectral function $A(k_F, E)$ (thin line) is obtained by symmetrizing the ARPES spectrum (dots); (middle) the ARPES spectrum beyond k_F (thick line) is simulated by applying a Fermi cutoff on a shifted replica (thin line) of $A(k_F, E)$. The finite intensity at E_F contrasts with the usual picture of a weakly interacting Fermi liquid (bottom).

pendicular to the layers, did not show any dispersion, and confirmed the quasi-two-dimensional nature of the electronic states. The diffuse intensity spread across most of the Brillouin zone (BZ) at ~ 0.5 eV anticipates the backfolding of the Ta band observed below T_{MI} (see below), and can be considered a precursor of the transition. As noticed before,¹⁴ the Fermi level crossing is not sharply defined, and some intensity is observed at E_F between k_F and Γ . The “fuzziness” of the Ta *d* band at RT has been ascribed to the finite size of the coherent CDW domains.¹³ Recent ARPES data on the related compound 1T-TaSe₂ (Ref. 17) suggest that correlations also play a role, namely near the Fermi surface, where the spectral function exhibits broad incoherent sidebands, condensing into sharp peaks at low temperature. Something similar happens here, as shown qualitatively in Fig. 1(b). We determined the spectral function for $k=k_F$ (top) by symmetrizing the measured spectrum to remove the Fermi cutoff: $A(k_F, E) \propto I(k_F, E) + I(k_F, -E)$. It exhibits a small peak at E_F and a broad *incoherent* tail. Between Γ and k_F , the QP energy lies above, but still close to, E_F , and it is reasonable to assume that $A(k, E)$ is satisfactorily described by a shifted replica of $A(k_F, E)$ (middle; thin line). Even after multiplication by a Fermi function, the broad incoherent tail yields a large ARPES signal at E_F (middle; thick line). This contrasts with the usual picture of a Fermi level crossing in a weakly interacting Fermi liquid (bottom). The blurred Fermi surface of Fig. 1(a) is therefore a consequence of a shallow band maximum at Γ , and of an unusually broad intrinsic spectral line shape which anticipates the formation of a low-temperature coherent state.

Changes in the band structure below the MI transition are illustrated by the ARPES intensity map of Fig. 2. The coherent CDW potential splits the occupied part of the Ta *d* band into subbands at ~ 1 eV, ~ 0.5 eV, and around E_F . The latter is further split by electronic correlations which drive the MI transition.⁹ The gap at E_F and the sharp Hubbard subband at

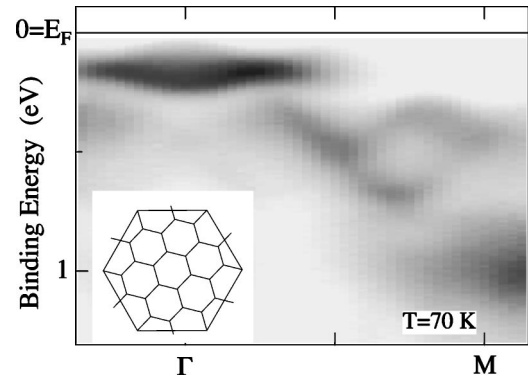


FIG. 2. ARPES intensity map of 1T-TaS₂ measured in the Mott insulating state (70 K). The spectral weight is concentrated along the main band, but superlattice (shadow) bands are visible, namely around 0.5 eV. The inset shows the original and the CDW-reconstructed Brillouin zones.

~ 0.2 eV around Γ are the hallmarks of the insulating state. Formally, the whole band structure should be folded back into the reduced Brillouin zone (BZ') of the $\sqrt{13} \times \sqrt{13}$ reconstructed structure. However, the spectral weight distribution in reciprocal space is controlled not only by symmetry, but also by the strength of the scattering potential.¹⁸ Therefore, the main band still carries most of the weight in the CDW phase, and only little intensity is transferred to the superlattice or “shadow” bands, which have not been observed so far. Faint shadows can nonetheless be identified, namely at ~ 0.5 eV, on high-quality surfaces (Fig. 2). These, and the gap feature discussed below, are quite sensitive to microscopic disorder and defects which are known to destroy the coherence of the CDW, and inhibit the MI transition.¹⁴ A detailed analysis shows that the shadow bands do exhibit the CDW periodicity.¹⁹

Qualitatively new insight is obtained by a closer investigation of the ARPES intensity distribution. First of all, the data show that the occupied Hubbard subband exhibits a definite (~ 70 meV) dispersion. Secondly, it is clear from Fig. 2 that some intensity spreads into the Mott gap. A second derivative plot [Fig. 3(a)], which enhances the visibility of weak features, reveals that this spectral weight is highly structured. The weaker band has a maximum at Γ , immedi-

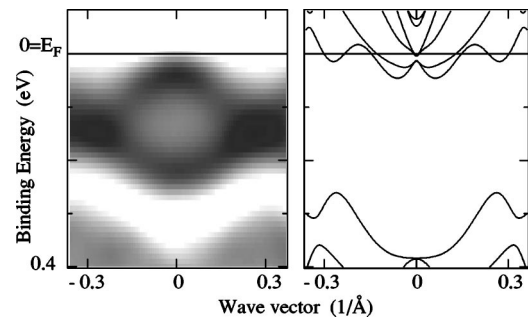


FIG. 3. (a) (left) Close-up of the Hubbard band from Fig. 2. The second derivative of the intensity is shown to enhance the weak shadow band with a maximum at Γ . (b) (right) Tight-binding band structure for a hypothetical metallic distorted phase around Γ .

ately below E_F , and its dispersion mirrors that of the Hubbard band. Within the accuracy of our determination of the “fuzzy” Fermi crossing in Fig. 1, the two bands cross at or very close to k_F . The weaker band certainly does not belong to the unperturbed band structure of 1T-TaS₂.^{10,15,16} Its intensity and dispersion identify it as a shadow resulting from backfolding the Hubbard band, but the corresponding periodic scattering potential remains to be identified. The CDW cannot provide the required periodicity. This can be easily verified by backfolding the metallic Ta d_{z^2} band into BZ’ (not shown). More accurately, a tight-binding model of the modulated structure can be set up for the CDW phase.¹⁰ It describes, in the absence of electronic correlations, a hypothetical distorted metallic phase. The result [Fig. 3(b)] excludes downward dispersing bands with the required periodicity at Γ , in proximity of the Fermi surface. The shadow band of Fig. 3(a) therefore reflects a distinct order parameter in the Mott insulating phase of 1T-TaS₂. Structural probes (x-ray diffraction, transmission electron microscopy, low-energy electron diffraction) give no indications of transitions to new ordered phases with periodicity larger than that of the CDW. Therefore, the new periodicity in the QP dispersion only indicates local order with a finite coherence length. The order parameter must fluctuate in space and time. This is consistent with the little spectral weight in the shadow band.

What is the nature of the underlying ordered state? The observation [Fig. 3(a)] of a zone boundary at $\sim k_F$ is reminiscent of an electronic instability (charge- or spin-density wave) driven by favorable nesting properties of the Fermi surface.¹ The negative results of standard diffraction experiments suggest that the spin degrees of freedom could be especially relevant. However, the soundness of such a weak-coupling scenario is not obvious. On one hand, detailed studies of the Fermi surface of metallic 1T-TaS₂²⁰ could not identify clear nesting vectors. On the other hand, the reconstructed Fermi surface of the distorted phase [Fig. 3(b) and Ref. 10] is quite complex, with many bands crossing E_F . Even if most of those bands carry very little spectral weight, it is not clear that nesting at k_F should produce the large enhancement of the susceptibility required to produce an instability.¹ Finally, the large lattice distortions, the broad ARPES line shape, and the occurrence of a Mott transition indicate that interactions are strong in this material, and that a strong-coupling description of the ordered phase may be more appropriate.²¹

We have explored the occurrence of possible ordered phases by a local, strong-coupling approach. In the absence of detailed knowledge of the relevant effective parameters of the strongly correlated insulating phase, we have decided to concentrate on the minimal model expected to exhibit the right physics. In this phenomenological model, we replace the 13 Ta atoms unit cell by one orbital which has an effective hopping amplitude $-t$ from one unit cell to another, and a “molecular” on-site repulsion U . This one-band Hubbard model on the triangular lattice is expected to undergo a Mott MI transition at half-filling at a critical value of $U/t \sim 10$.^{22,23} There is strong numerical evidence that this Mott insulating state has the same long-range order as the classical Néel ground state,²⁴ even if frustration is present. The classical

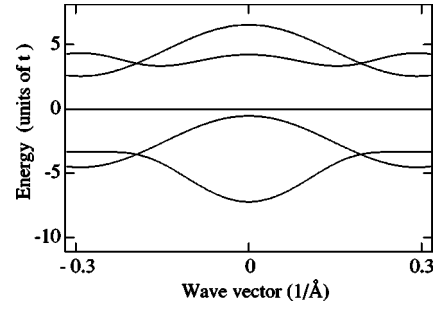


FIG. 4. The Hartree-Fock energy bands for the Néel state around Γ . The on-site interaction was set to $U=8t$.

Néel state splits the lattice into three sublattices where the spins on each sublattice are ferromagnetically aligned and the orientation of the spins differs by $\pm 2\pi/3$ from one sublattice to another. We describe this Néel state within Hartree-Fock theory.²³ Defining the mean-field magnetic moments as $S_i = \sum_{\sigma\sigma'} \langle c_{i\sigma}^\dagger \sigma_{\sigma\sigma'} c_{i\sigma'} \rangle$, where σ is a vector containing the Pauli matrices, the Hartree-Fock Hamiltonian for the half-filled Hubbard model reads

$$H = -t \sum_{\langle i,j \rangle \sigma} (c_{i\sigma}^\dagger c_{j\sigma} + \text{H.c.}) - \frac{U}{2} \sum_{i\sigma\sigma'} S_i \cdot c_{i\sigma}^\dagger \sigma_{\sigma\sigma'} c_{i\sigma'} + \frac{U}{2} \sum_{i\sigma} c_{i\sigma}^\dagger c_{i\sigma} + \frac{U}{4} \sum_i (|S_i|^2 - 1). \quad (1)$$

For the expectation values, we make the ansatz $\langle S_{xi} \rangle + i \langle S_{yi} \rangle = m \exp(i\mathbf{Q} \cdot \mathbf{R}_i)$ with $\mathbf{Q} = (4\pi/3, 0)$. The magnetization m is determined self-consistently. The results of this calculation are shown in Fig. 4.

We plot the six (partially degenerate) Hartree-Fock energy bands along the high-symmetry $\Gamma M'$ direction of BZ'. The calculated band structure accounts for the known experimental facts in 1T-TaS₂ in two important respects: (i) it describes a correlated insulator, with an energy gap which, albeit smaller than the Coulomb energy U , is determined by U ; (ii) near Γ the occupied subbands are split, and disperse with opposite phases, as the ARPES bands of Fig. 3. We consider this overall agreement a strong indication that, even if no magnetic long-range order has been so far established in 1T-TaS₂, the physics in the CDW phase could be strongly influenced by such antiferromagnetic fluctuations. To go in a meaningful way beyond this good but not fully quantitative agreement will require having a better understanding of the insulating phase either from LDA+ U estimates of the effective parameters²⁵ or from experimental evidence of magnetic fluctuations, and is thus left for future investigation.

In summary, we have shown that ARPES data on the quasi-two-dimensional Mott insulator 1T-TaS₂ carry characteristic traces of two distinct order parameters. The first describes the CDW state which drives the MI transition. The second is a fluctuating order parameter which we associate with the spin degrees of freedom of Ta d electrons localized at the center of the “star of David” units of the CDW. A phenomenological approach based on a Hubbard model cal-

ulation reproduces remarkably well the qualitatively new features of the ARPES experiment. Although we are confident that the model captures the essential physics of the problem, more detailed calculations are required to interpret quantitatively the data, namely the distribution of spectral weight between the main and superlattice bands. The present findings should also stimulate new investigations of a possible low-temperature phase transition, namely by neutron

diffraction and magnetic x-ray scattering experiments, which are specifically sensitive to magnetic order.

This work has been supported by the Swiss National Science Foundation through the MaNEP NCCR. We thank Professor H. Fukuyama for stimulating suggestions, and acknowledge correspondence with F. del Dongo and P. Besucov.

-
- ¹G. Grüner, *Density Waves in Solids* (Addison-Wesley, Reading, MA, 1994).
 - ²M. Imada, A. Fujimori, and Y. Tokura, *Rev. Mod. Phys.* **70**, 1039 (1998).
 - ³For a review in 2D, see, e.g., E. Dagotto, *Rev. Mod. Phys.* **66**, 763 (1994).
 - ⁴For a review in 1D, see, e.g., J. Voit, *Rep. Prog. Phys.* **58**, 977 (1995).
 - ⁵See, e.g., A. Georges, G. Kotliar, W. Krauth, and M. J. Rozenberg, *Rev. Mod. Phys.* **68**, 13 (1996).
 - ⁶For a recent review, see G. Misguich and C. Lhuillier, e-print cond-mat/0310405.
 - ⁷A. Damascelli, Z. Hussain, and Z.-X. Shen, *Rev. Mod. Phys.* **75**, 473 (2003).
 - ⁸J. A. Wilson, F. J. DiSalvo, and S. Mahajan, *Adv. Phys.* **24**, 117 (1975).
 - ⁹P. Fazekas and E. Tosatti, *Philos. Mag. B* **39**, 229 (1979).
 - ¹⁰N. V. Smith, S. D. Kevan, and F. J. DiSalvo, *J. Phys. C* **18**, 3175 (1985).
 - ¹¹R. A. Pollak, D. E. Eastman, F. J. Himpsel, P. Heimann, and B. Reihl, *Phys. Rev. B* **24**, 7435 (1981).
 - ¹²R. Manzke, T. Buslaps, B. Pfalzgraf, M. Skibowski, and O. Anderson, *Europhys. Lett.* **8**, 195 (1989).
 - ¹³R. Claessen, B. Burandt, H. Carstensen, and M. Skibowski, *Phys. Rev. B* **41**, 8270 (1990).
 - ¹⁴F. Zwick, H. Berger, I. Vobornik, G. Margaritondo, L. Forró, C. Beeli, M. Onellion, G. Panaccione, A. Taleb-Ibrahimi, and M. Grioni, *Phys. Rev. Lett.* **81**, 1058 (1998).
 - ¹⁵Y. Aiura, I. Hase, H. Bando, K. Yagi-Watanabe, K. Ozawa, T. Iwase, Y. Nishihara, O. Shiino, M. Oshima, M. Kubota, and K. Ono, *Phys. Rev. Lett.* **91**, 256404 (2003).
 - ¹⁶M. Bovet, S. van Smaalen, H. Berger, R. Gaal, L. Forró, L. Schlapbach, and P. Aebi, *Phys. Rev. B* **67**, 125105 (2003).
 - ¹⁷L. Perfetti, A. Georges, S. Florens, S. Biermann, S. Mitrovic, H. Berger, Y. Tomm, H. Höchst, and M. Grioni, *Phys. Rev. Lett.* **90**, 166401 (2003).
 - ¹⁸J. Voit, L. Perfetti, F. Zwick, H. Berger, G. Margaritondo, G. Grüner, H. Höchst, and M. Grioni, *Science* **290**, 501 (2000).
 - ¹⁹L. Perfetti, Ph.D. thesis, EPFL, Lausanne, 2003.
 - ²⁰R. L. Withers and J. A. Wilson, *J. Phys. C* **19**, 4809 (1986).
 - ²¹P. Majumdar and H. R. Krishnamurthy, *Phys. Rev. Lett.* **73**, 1525 (1994).
 - ²²M. Capone, L. Capriotti, F. Becca, and S. Caprara, *Phys. Rev. B* **63**, 085104 (2001); C. J. Gazza, A. E. Trumper, and H. A. Cecatto, *J. Phys.: Condens. Matter* **6**, L625 (1994).
 - ²³H. R. Krishnamurthy, C. Jayaprakash, S. Sarker, and W. Wenzel, *Phys. Rev. Lett.* **64**, 950 (1990); C. Jayaprakash, H. R. Krishnamurthy, S. Sarker, and W. Wenzel, *Europhys. Lett.* **15**, 625 (1991); K. Machida and M. Fujita, *Phys. Rev. B* **42**, 2673 (1990); C. Pinettes and C. Lacroix, *Solid State Commun.* **85**, 565 (1993).
 - ²⁴B. Bernu, C. Lhuillier, and L. Pierre, *Phys. Rev. Lett.* **69**, 2590 (1992); L. Capriotti, A. E. Trumper, and S. Sorella, *ibid.* **82**, 3899 (1999).
 - ²⁵V. I. Anisimov, J. Zaanen, and O. K. Andersen, *Phys. Rev. B* **44**, 943 (1991).